

Plasminogen Activator Inhibitor-1 Promotes Neutrophil Infiltration and Tissue Injury on Ischemia–Reperfusion

Marc Praetner,* Gabriele Zuchtriegel,* Martin Holzer, Bernd Uhl, Johanna Schaubächer, Laura Mittmann, Matthias Fabritius, Robert Fürst, Stefan Zahler, Dominik Funken, Maximilian Lerchenberger, Andrej Khandoga, Sandip Kanse, Kirsten Lauber, Fritz Krombach, Christoph A. Reichel

Objective—Ischemia–reperfusion (I/R) injury significantly contributes to organ dysfunction and failure after myocardial infarction, stroke, and transplantation. In addition to its established role in the fibrinolytic system, plasminogen activator inhibitor-1 has recently been implicated in the pathogenesis of I/R injury. The underlying mechanisms remain largely obscure.

Approach and Results—Using different in vivo microscopy techniques as well as ex vivo analyses and in vitro assays, we identified that plasminogen activator inhibitor-1 rapidly accumulates on microvascular endothelial cells on I/R enabling this protease inhibitor to exhibit previously unrecognized functional properties by inducing an increase in the affinity of $\beta 2$ integrins in intravascularly rolling neutrophils. These events are mediated through low-density lipoprotein receptor–related protein-1 and mitogen-activated protein kinase–dependent signaling pathways that initiate intravascular adherence of these immune cells to the microvascular endothelium. Subsequent to this process, extravasating neutrophils disrupt endothelial junctions and promote the postischemic microvascular leakage. Conversely, deficiency of plasminogen activator inhibitor-1 effectively reversed leukocyte infiltration, microvascular dysfunction, and tissue injury on experimental I/R without exhibiting side effects on microvascular hemostasis.

Conclusions—Our experimental data provide novel insights into the nonfibrinolytic properties of the fibrinolytic system and emphasize plasminogen activator inhibitor-1 as a promising target for the prevention and treatment of I/R injury.

Visual Overview—An online [visual overview](#) is available for this article. (*Arterioscler Thromb Vasc Biol.* 2018;38:829-842. DOI: 10.1161/ATVBAHA.117.309760.)



Key Words: fibrinolysis ■ leukocyte ■ mitogen-activated protein kinases ■ plasminogen activator inhibitor 1 ■ reperfusion injury

Ischemia–reperfusion (I/R) injury is one of the major mechanisms behind organ dysfunction and failure after myocardial infarction, stroke, and transplantation. In the postischemic inflammatory response, leukocytes accumulate in the microvasculature and compromise reperfusion of the injured tissue. Extravasating leukocytes release reactive oxygen species, cytokines, and proteases, which promotes microvascular leakage and amplifies the ischemic tissue injury.^{1,2} Concomitantly, leukocytes phagocytose apoptotic/necrotic cells and produce anti-inflammatory factors that actively contribute to tissue regeneration and healing³ collectively emphasizing leukocytes as key players in the pathogenesis of I/R injury.

Fibrinolysis is a fundamental biological process that enables the maintenance of tissue perfusion by preventing clot formation in blood vessels. Plasmin is the principal effector protease in the fibrinolytic system mediating the dissolution of fibrin polymers. Its zymogen form, plasminogen, is activated by tPA (tissue-type plasminogen activator) and, to a much lesser degree, by urokinase-type plasminogen activator. Beyond their established role in the fibrinolytic system, these serine proteases have previously been documented to contribute to different biological processes,^{4–7} including the regulation of distinct steps in leukocyte recruitment to postischemic tissue.^{8–11}

Plasminogen activator inhibitor-1 (PAI-1) is the principal inhibitor of the plasminogen activators limiting exaggerated fibrinolytic activity. Secreted by hepatocytes and microvascular endothelial cells, PAI-1 is primarily found circulating

See accompanying editorial on page 695

Received on: June 2, 2017; final version accepted on: January 15, 2018.

From the Walter Brendel Centre of Experimental Medicine (M.P., G.Z., M.H., B.U., J.S., L.M., M.F., D.F., M.L., A.K., F.K., C.A.R.), Department of Otorhinolaryngology (G.Z., M.H., B.U., C.A.R.), Head and Neck Surgery (M.P.), Pharmaceutical Biology, Department of Pharmacy, Center for Drug Research (S.Z.), Department of Surgery (D.F., M.L., A.K.), and Department of Radiation Oncology (K.L.), Ludwig-Maximilians-Universität München, Munich, Germany; Department of Psychiatry and Psychotherapy, University Clinic, Friedrich-Alexander-University of Erlangen-Nuremberg, Germany (M.P.); Institute of Pharmaceutical Biology, Goethe University Frankfurt, Germany (R.F.); and Institute of Basic Medical Sciences, University of Oslo, Norway (S.K.).

*These authors contributed equally to this article.

The online-only Data Supplement is available with this article at <http://atvb.ahajournals.org/lookup/suppl/doi:10.1161/ATVBAHA.117.309760/-/DC1>.

Correspondence to Christoph A. Reichel, Priv-Doz Dr med, Department of Otorhinolaryngology and Walter Brendel Centre of Experimental Medicine, Ludwig-Maximilians-Universität München, Marchioninistr. 15, D-81377 Munich, Germany. E-mail christoph.reichel@med.uni-muenchen.de

© 2018 American Heart Association, Inc.

Arterioscler Thromb Vasc Biol is available at <http://atvb.ahajournals.org>

DOI: 10.1161/ATVBAHA.117.309760

Nonstandard Abbreviations and Acronyms

ICAM	intercellular adhesion molecule
I/R	ischemia–reperfusion
LRP-1	low-density lipoprotein receptor–related protein-1
MAPK	mitogen-activated protein kinases
PAI-1	plasminogen activator inhibitor-1
RAP	receptor-associated protein
VCAM	vascular cell adhesion molecule

in the blood. In addition to its well-known antifibrinolytic properties, also PAI-1 has been implicated in nonfibrinolytic processes, such as cell adhesion and migration.^{4,12,13} In the context of I/R, elevated levels of PAI-1 have been reported to be an independent risk factor for ischemic cardiovascular events.^{14–17} The functional role of PAI-1 in the pathogenesis of I/R injury, however, remained largely unclear.

In the present study, we demonstrate that PAI-1 plays a pivotal role during the initiation of the postischemic inflammatory response by directing neutrophils to the site of injury: Subsequent to a rapid immobilization on the postischemic microvascular endothelium, this protease inhibitor induces affinity changes of $\beta 2$ integrins in intravascularly rolling neutrophils which promote the accumulation of these immune cells in the reperfused tissue. Interfering with these, PAI-1–dependent events effectively attenuated leukocyte infiltration, microvascular dysfunction, and tissue injury on experimental I/R without exhibiting side effects on microvascular hemostasis. Our experimental data provide novel insights into the nonfibrinolytic properties of the fibrinolytic system and propose the inhibition of PAI-1 as a promising strategy for the prevention and treatment of I/R injury.

Materials and Methods

Animals

Male C57BL/6J mice were purchased from Charles River (Sulzfeld, Germany). PAI-1–deficient mice (backcrossed for >10 generations on a C57BL/6J background) were generated at the Jackson Laboratory (Bar Harbor) and purchased from Charles River. All experiments were performed with male mice at the age of 10–12 weeks. Animals were held under standard laboratory conditions with free access to animal chow and water. All experiments were performed according to the German legislation for the protection of animals (approved by the government of Upper Bavaria).

Surgical Procedures

M. Cremaster Assay

The surgical preparation of the cremaster muscle was performed as originally described by Baez¹⁸ with minor modifications. Mice were anesthetized using a ketamine/xylazine mixture (100 mg/kg ketamine and 10 mg/kg xylazine), administered by IP injection. The left femoral artery was cannulated in a retrograde manner (polyethylene-10, inner diameter 0.28 mm; Portex, Hythe, UK) for administration of microspheres and drugs. The right cremaster muscle was exposed through a ventral incision of the scrotum. The muscle was opened ventrally in a relatively avascular zone, using careful electrocautery to stop any bleeding and spread over the transparent pedestal of a custom-made microscopy stage. Epididymis and testicle were detached from the cremaster muscle and replaced into the abdominal cavity. Throughout the procedure and after surgical preparation during in vivo microscopy, the muscle was superfused with warm-buffered saline.

Hepatic I/R Injury

Warm ischemia of the left liver lobe was induced for 90 minutes by reversible clamping of the supplying vessels as described previously.⁹ Tissue and blood samples were taken at the end of the experiment after 120 minutes of reperfusion. Blood samples were immediately centrifuged at 2000g for 10 minutes and stored at -80°C . Serum aspartate aminotransferase (AST) and alanine transaminase (ALT) activities were measured with an automated analyzer (Hitachi 917; Roche-Boehringer Mannheim, Co, Germany) using standardized test systems (HiCo GOT and HiCo GPT; Roche-Boehringer Mannheim, Co).

In Vivo Microscopy

The setup for in vivo microscopic analyses of leukocyte recruitment and microvascular permeability was centered around an AxioTech-Vario 100 Microscope (Zeiss MicroImaging GmbH, Göttingen, Germany), equipped with a Colibri LED light source (Zeiss MicroImaging GmbH) for fluorescence epi-illumination microscopy. For fluorescein isothiocyanate (FITC)–dextran excitation or reflected oblique light illumination, 470 or 625 nm were used, respectively. Light was directed onto the specimen via filter set 62 high efficiency (HE; Zeiss MicroImaging GmbH) fitted with dichroic and emission filters (TFT 495+610 [HE]; tunable bandpass 527+LP615 [HE]). Microscopy images were obtained with an AxioCam Hsm digital camera using a $\times 20$ water immersion lens (0.5 numeric aperture [NA]; Zeiss MicroImaging GmbH). Reflected light oblique transillumination was obtained by positioning a mirroring surface (reflector) directly below the specimen and tilting its angle relative to the horizontal plane. The reflector consisted of a round cover glass (thickness, 0.19–0.22 mm; diameter, 11.8 mm), which was coated with aluminum vapor (Freichel, Kaufbeuren, Germany) and brought into direct contact with the overlying specimen as described previously.¹⁹

The set-up for in vivo microscopic analyses of phototoxic injury–induced microvascular thrombosis was centered around an Olympus BX 50 upright microscope (Olympus Microscopy, Hamburg, Germany). Light from a 75-W xenon source was narrowed to a near monochromatic beam of a wavelength of 488 nm by a galvanometric scanner (Polychrome II; TILL Photonics, Gräfelfing, Germany) and directed onto the specimen via a FITC filter cube equipped with dichroic and emission filters (DCLP 500, LP515; Olympus Microscopy). Microscopic images were obtained with Olympus water immersion lenses ($\times 20$ /NA 0.5 and $60\times$ /NA 0.9), recorded with a charge-coupled device camera (IMAGO S/N 382KLO345; TILL Photonics GmbH, Gräfelfing, Germany) and subjected to digital image analysis (TILLvisION 4.0; TILL Photonics GmbH).

For measurement of centerline blood flow velocity, green fluorescent microspheres (0.96 μm diameter; Molecular Probes, Leiden, The Netherlands) were injected via the femoral artery catheter, and their passage through the vessels of interest was recorded in both microscopy set-ups employed, using the FITC filter cube under appropriate stroboscopic illumination (exposure, 1 ms; cycle time, 10 ms; $l=488$ nm), integrating video images for sufficient time (0.80 ms) to allow for the recording of several images of the same bead on one frame. Beads that were flowing freely along the centerline of the vessels were used to determine blood flow velocity.

Quantification of Leukocyte Kinetics and Microhemodynamic Parameters

Off-line analysis of parameters describing the sequential steps of leukocyte extravasation was performed with AxioVision 4.6 software (Zeiss MicroImaging GmbH). ImageJ software (National Institutes of Health, Bethesda, MD) was used for further image processing and analysis. Rolling leukocytes were defined as those moving slower than the associated blood flow and quantified for 30 seconds. Firmly adherent cells were determined as those resting in the associated blood flow for >30 seconds and related to the luminal surface per 100- μm vessel length. Transmigrated cells were counted in regions of interest, covering 75 μm on both sides of a vessel >100 μm vessel length. By measuring the distance between several images of one fluorescent

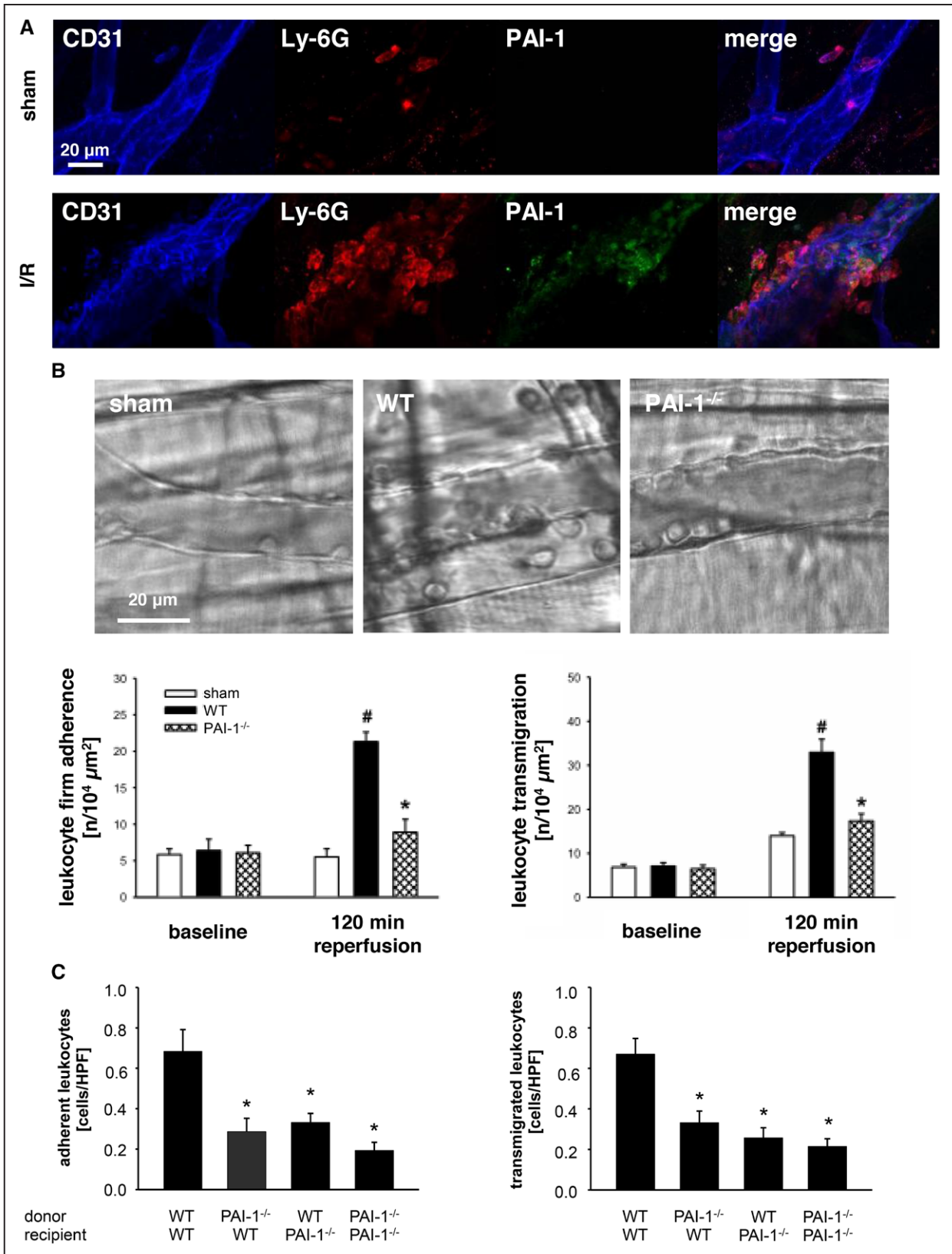


Figure 1. Role of plasminogen activator inhibitor-1 (PAI-1) for postischemic leukocyte responses. Using confocal microscopy, distribution of PAI-1 was analyzed in postcapillary venules of the cremaster muscle of sham-operated wild-type (WT) mice or of WT mice undergoing ischemia-reperfusion (I/R; 30/120 min) as detailed in Material and Methods in the [online-only Data Supplement](#). **A**, Representative images of CD31-positive (blue; endothelial cells, leukocytes) and Ly-6G-positive (red; neutrophils) cells, as well as of PAI-1 (green). Leukocyte recruitment to the mouse cremaster muscle was analyzed by in vivo microscopy after 30 min of ischemia and 120 min of reperfusion as detailed in Material and Methods in the [online-only Data Supplement](#). **B**, Representative in vivo microscopy images and (*Continued*)

bead under stroboscopic illumination, centerline blood flow velocity was determined. From measured vessel diameters and centerline blood flow velocity, apparent wall shear stress was calculated, assuming a parabolic flow velocity profile over the vessel cross-section.

Cell Transfer Experiments

To investigate the contribution of leukocyte and non-leukocyte PAI-1 to postischemic leukocyte responses, a cell-transfer technique was used as described previously.⁹ Leukocytes were isolated from donor mice by flushing the femur and tibia bones with PBS. Cells were then sieved and counted, resuspended in PBS containing BSA (0.25%), and incubated with calcein-AM (10 $\mu\text{mol/L}$ final concentration at 37°C for 30 minutes). After 2 washes, the cells were injected intravenously into recipient mice via the right jugular vein (10^7 cells/mouse) 120 minutes before the surgical preparation. Fluorescent cells were counted in 175 high power fields per animal; this being equivalent to the total quantifiable area of an exteriorized cremaster muscle in the present studies. Results are shown as the number of adherent or transmigrated calcein-labeled cells/high power field.

Reagents

Recombinant mouse PAI-1 and human RAP (Molecular Innovations, Novi, MI). Anti-LRP-1 antibody ($\alpha 2$ -M-R/LRP1/CD91; polyclonal; BioMac, Leipzig, Germany). Neutrophil-depleting anti-Ly-6G monoclonal antibody (clone 1A8; 100 μg IV 24 and 6 hours before induction of inflammation; BD Biosciences, San Jose, CA). FITC dextran (150 kDa; Sigma-Aldrich, Deisenhofen, Germany).

Experimental Groups

Animals were assigned to the following groups: sham-operated wild-type (WT) mice as well as WT mice, PAI-1^{-/-} mice, and WT mice treated 5 minutes before reperfusion with anti-LRP-1 antibody, the PAI-1 inhibitor TM5275 (40 mg/kg body weight; IA), or isotype control/vehicle undergoing I/R (30/120 min; n=4–6 each group). Moreover, leukocyte responses were analyzed in the cremaster muscle of WT mice receiving fluorescent leukocytes from WT or PAI-1^{-/-} donors and of PAI-1^{-/-} mice receiving fluorescent leukocytes from WT donors undergoing I/R (30/120 min; n=5 each group). In another set of experiments, WT mice received PBS (200 μL ; supplemented with 0.01 % BSA), different doses of murine (active) PAI-1 (0.01, 0.1, 1.0 μg ; diluted in 200 μL PBS supplemented with 0.01% BSA), or latent (inactive) PAI-1 (1.0 μg ; diluted in 200 μL PBS supplemented with 0.01% BSA) administered by intrascrotal injection (n=4 each group). Additional experiments were performed in WT mice receiving RAP, anti-LRP-1 antibody, or drug vehicle/isotype control undergoing stimulation with recombinant murine PAI-1 (1.0 μg intrascrotal; n=5 each group). Further experiments were performed in WT mice either pretreated with the neutrophil-depleting monoclonal anti-Ly-6G antibody 1A8 or isotype control undergoing stimulation with recombinant murine PAI-1 (1.0 μg intrascrotal; n=6 each group). In additional experiments, phototoxic injury-induced thrombosis (see below) was induced in WT and PAI-1^{-/-} mice (n=5 each group). In a final set of experiments, warm hepatic I/R (90/120 minutes) was induced in sham-operated WT mice, as well as in WT mice, in PAI-1^{-/-} mice, or in WT mice treated with TM5275 or vehicle (n=4–6 each group).

I/R Injury

For the analysis of I/R-elicited leukocyte responses, 3 postcapillary vessel segments in a central area of the spread-out cremaster muscle

were randomly chosen among those that were at least 150 μm away from neighboring postcapillary venules and did not branch over a distance of at least 150 μm . After having obtained baseline recordings of leukocyte rolling, firm adhesion, and transmigration in all 3 vessel segments, ischemia was induced by clamping all supplying vessels at the basis of the cremaster muscle using a vascular clamp (Martin, Tuttlingen, Germany) as described previously.⁹ Stagnancy of blood flow was then verified by in vivo microscopy. After 30 minutes of ischemia, the vascular clamp was removed, and reperfusion was restored for 120 minutes. Measurements, which took about 5 minutes, respectively, were repeated at 60 and 120 minutes after the onset of reperfusion.

After in vivo microscopy, tissue samples of the cremaster muscle were taken for immunohistochemistry. Blood samples were collected by cardiac puncture for the determination of systemic leukocyte counts using a Coulter ACT Counter (Coulter, Corp, Miami, FL). Anesthetized animals were then killed by exsanguination.

Neutrophil Depletion

Depletion of neutrophils was accomplished by using a rat antimouse monoclonal antibody (anti-Ly-6G monoclonal antibody; clone 1A8; 100 μg IV; 24 and 6 hours before the experiment). Successful neutrophil depletion was confirmed by flow cytometry analysis and defined as a reduction of circulating neutrophils by >95% compared with animals treated with an isotype control antibody.

Microvascular Permeability

As a measure of microvascular permeability, leakage of the macromolecule FITC dextran (5 mg in 0.15 mL saline, IA, Mr [relative molecular mass] 150 kDa) was analyzed as described previously.⁹ Thirty minutes after application of FITC dextran, 6 randomly chosen postcapillary vessel segments and the surrounding perivascular tissue was excited at 488 nm, and emission 515 nm was recorded by an AxioCam Hsm digital camera (Zeiss MicroImaging GmbH, Germany) using an appropriate emission filter (LP 515). Mean gray values of fluorescence intensity were measured by digital image analysis (ImageJ Software; National Institutes of Health) in 6 randomly selected regions of interest (50 \times 50 μm^2), localized 50 μm distant from the postcapillary venule under investigation.

Macromolecular Permeability of Human Microvascular Endothelial Cell Lines

The human dermal microvascular endothelial cell line CDC/EU.HMEC-1 was kindly provided by the US Centers for Disease Control and Prevention (CDC; Atlanta, GA). Human microvascular endothelial cell lines (HMECs) are proven to preserve morphology, phenotype, and functionality of normal human microvascular ECs.²⁰ HMECs were cultured in endothelial growth medium (ECGM; Provitro, Berlin, Germany) containing 10% heat-inactivated fetal calf serum (Biochrom, Berlin, Germany), penicillin (100 U/mL)/streptomycin (100 $\mu\text{g}/\text{mL}$), and amphotericin B (0.25 $\mu\text{g}/\text{mL}$) at 37°C in humidified air with 5% CO₂.

HMECs were cultured on 12-well Transwell inserts (pore size 0.4 μm ; Corning, New York, NY). FITC dextran (40 kDa; 1 mg/mL; Sigma-Aldrich) was given to the upper compartment at $t=0$ minutes, and cells were treated as indicated. RAP (100 ng/mL) was applied 15 minutes before PAI-1. Samples were taken from the lower compartment at $t=60$ min. The fluorescence (λ_{ex} : 485 nm; λ_{em} : 535 nm)

Figure 1 Continued. quantitative data for intravascular adherence and transmigration of leukocytes (>85% Ly-6G–positive neutrophils) to the postischemic tissue in sham-operated WT mice and in WT or PAI-1–deficient mice undergoing I/R (mean \pm SEM for n=4 per group; # $P<0.05$, vs sham; * $P<0.05$, vs WT). Adherence and transmigration of calcein AM-labeled bone marrow leukocytes were quantified in the cremaster muscle after 30 min of ischemia and 120 min of reperfusion using in vivo fluorescence microscopy as detailed in Material and Methods in the [online-only Data Supplement](#). **C**, Results for WT mice receiving leukocytes from WT or PAI-1–deficient donors as well as for PAI-1–deficient mice receiving leukocytes from WT or PAI-1–deficient donors (mean \pm SEM for n=6 per group; * $P<0.05$, vs WT \rightarrow WT).

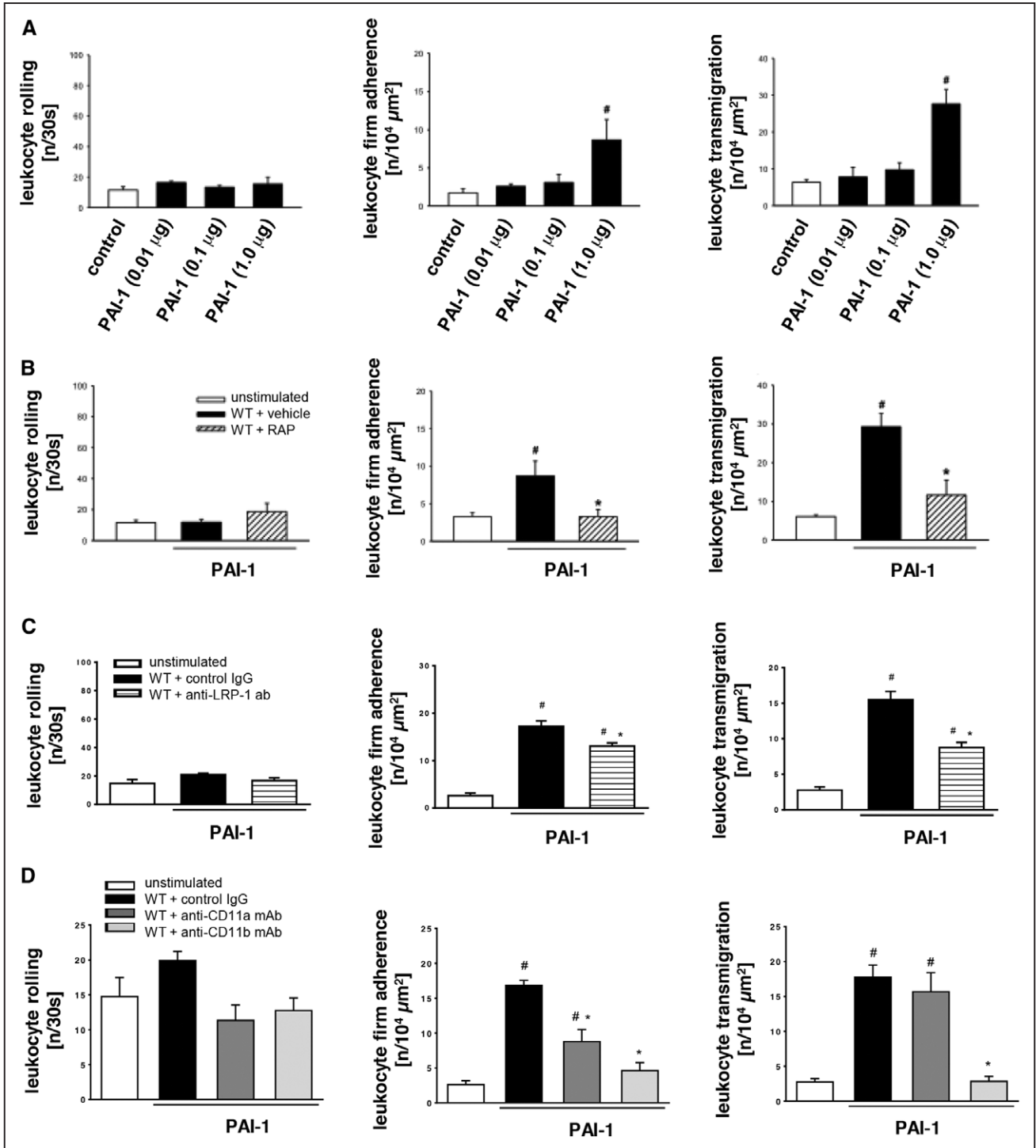


Figure 2. Mechanisms underlying plasminogen activator inhibitor-1 (PAI-1)-elicited leukocyte responses. Using in vivo microscopy on the cremaster muscle of WT mice, leukocyte recruitment was analyzed on intrascrotal injection of varying doses of recombinant murine PAI-1 or vehicle as detailed in Material and Methods in the [online-only Data Supplement](#). **A**, Quantitative data for intravascular rolling and firm adherence as well as transmigration of leukocytes (>85% Ly-6G-positive neutrophils) to the perivascular tissue. **B–D**, Quantitative data for intravascular rolling and firm adherence as well as transmigration of leukocytes obtained in wild-type (WT) mice receiving an intrarterial injection of RAP (receptor-associated protein), anti-LRP-1 (low-density lipoprotein receptor-related protein-1) Abs, anti-LFA-1 (lymphocyte function-associated antigen-1)/CD11a mAbs, anti-Mac-1/CD11b mAbs, or vehicle/isotype control as well as an intrascrotal injection of 1 μg PAI-1 (mean±SEM for n=5 per group; #P<0.05, vs control/unstimulated; *P<0.05, vs vehicle/isotype control).

increase of the samples was detected with a SpectraFluorPlus plate reader (Tecan, Crailsheim, Germany). All experiments were independently performed for at least 3 times.

Phototoxic Injury-Induced Thrombosis

Phototoxic injury-induced thrombosis was performed in cremasteric arterioles and venules as described earlier.²¹ Light intensity

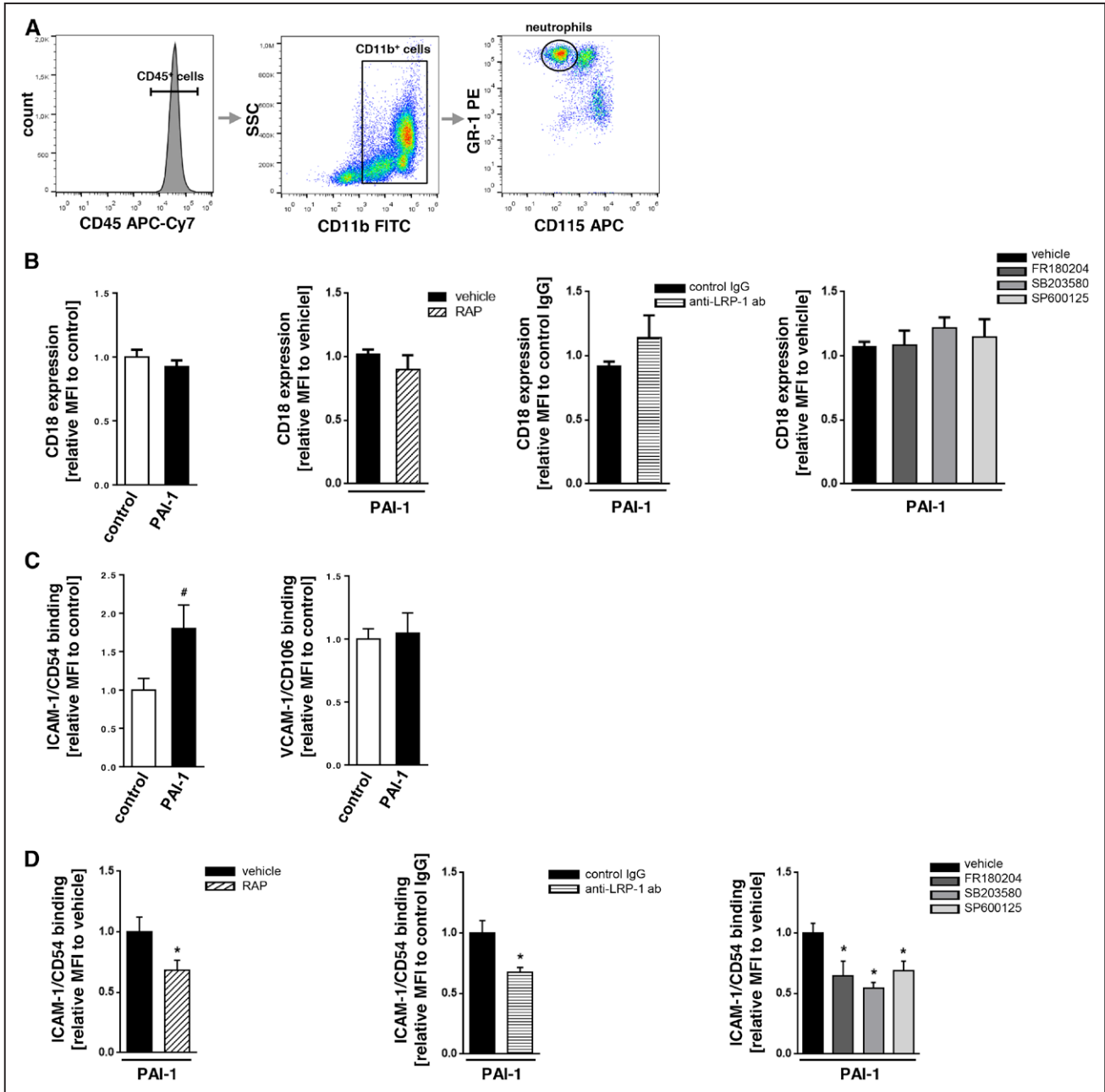


Figure 3. Effect of plasminogen activator inhibitor-1 (PAI-1) on activation of neutrophils. As a measure of conformational changes in neutrophil integrins, binding of intercellular adhesion molecule (ICAM)-1/CD54 or vascular cell adhesion molecule (VCAM)-1/CD106 was analyzed in neutrophils isolated from the peripheral blood of wild-type mice by multichannel flow cytometry as detailed in Material and Methods in the [online-only Data Supplement](#). **A**, Gating strategy for identifying neutrophils. **B**, Quantitative data for surface expression of CD18 and **(C and D)** for the binding of ICAM-1/CD54 or VCAM-1/CD106 to neutrophils pre-incubated with RAP (receptor-associated protein), anti-LRP-1 (low-density lipoprotein receptor-related protein-1) Abs, different mitogen-activated protein kinase (MAPK) inhibitors, or vehicle/isotype control Abs (mean±SEM for n=4–6 per group; [#]*P*<0.05, vs control; ^{*}*P*<0.05, vs vehicle/isotype control). APC indicates allophycocyanin; FITC, fluorescein isothiocyanate; and SSC, side-scattered light.

values were measured by a photodiode at 488 nm at the exit of the light source in each experiment before induction of thrombosis and maintained between 2.65 and 2.75 mA. After surgical preparation of the cremaster muscle, appropriate microvessels were chosen, centerline blood flow velocity was determined as described above, and, subsequently, FITC dextran was applied. Five minutes later, photoactivation was induced by exposing a vessel segment of 300 μm length to continuous epi-illumination with a wavelength of 488 nm using an Olympus water immersion lens (×60/NA 0.9). Thrombus

formation was quantified in one venule (30–50 μm in diameter) and in one arteriole (25–35 μm in diameter) per experiment. Onset time of thrombus formation is defined by the time when first platelets became adherent to the vessel wall. Cessation time of blood flow is defined as the time required for complete occlusion of the vessel. Occlusion time in vessels without complete occlusion until the end of the recording was considered 20 minutes for venules and 40 minutes for arterioles.

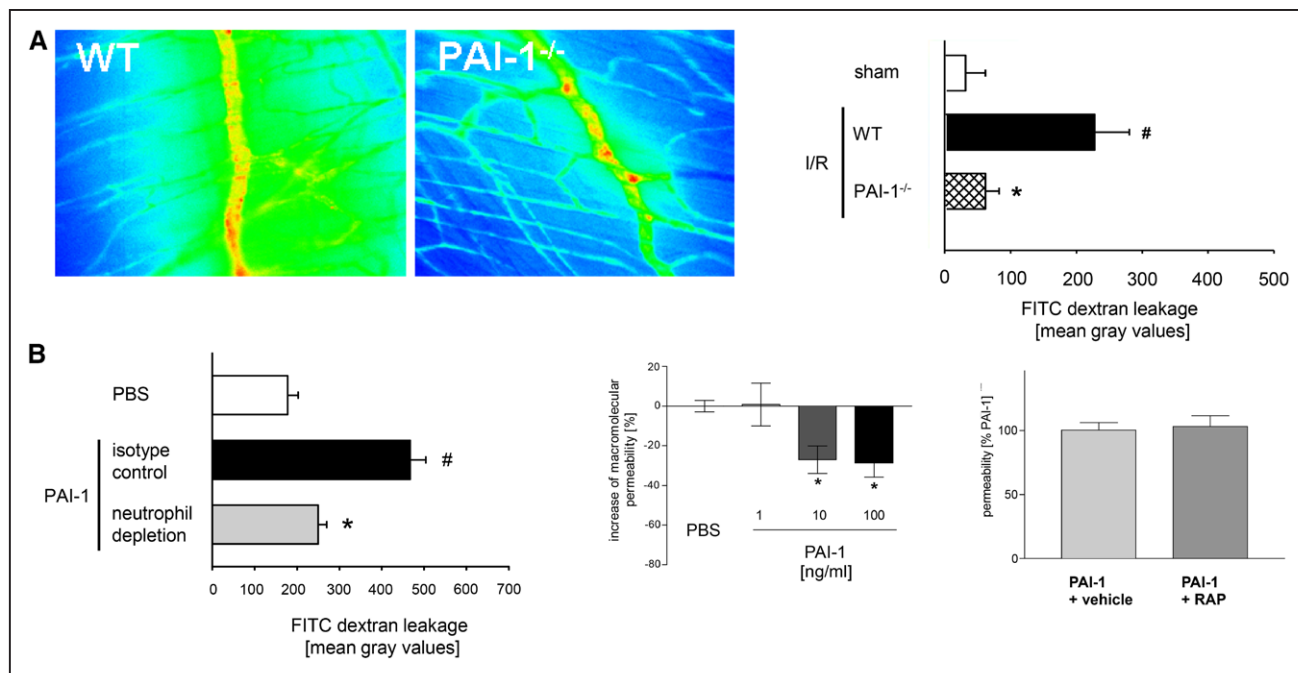


Figure 4. Role of plasminogen activator inhibitor-1 (PAI-1) for postischemic microvascular leakage. As a measure of microvascular leakage, extravasation of fluorescein isothiocyanate (FITC) dextran was analyzed in the cremaster muscle of wild-type (WT) mice by fluorescence in vivo microscopy as detailed in Material and Methods in the [online-only Data Supplement](#), representative images are shown (A). Panels show quantitative data for FITC dextran leakage in sham-operated WT mice as well as in WT or PAI-1-deficient mice undergoing I/R (30/150 min) and in unstimulated WT mice as well as in WT mice treated with neutrophil-depleting anti-Ly-6G mAbs or isotype control Abs undergoing intrascrotal stimulation with recombinant murine PAI-1 (B; mean \pm SEM for n=4–6 per group; # P <0.05, vs sham/PBS; * P <0.05, vs WT/vehicle/isotype control). Macromolecular permeability for FITC dextran was analyzed in vitro in confluent HMEC (human microvascular endothelial cell line-1) layers as detailed in Material and Methods in the [online-only Data Supplement](#). B, Quantitative data for cell layers exposed to varying doses of recombinant human PAI-1 as well as RAP (receptor-associated protein) or vehicle (mean \pm SEM for n=3–4 per group; * P <0.05, vs PBS).

Microvascular Fibrin(ogen) Deposition

Deposition of fibrin(ogen) on microvascular endothelial cells was determined in a separate set of experiments by in vivo fluorescence microscopy as demonstrated before with minor modifications.¹⁰ Briefly, Alexa 488-conjugated human fibrinogen (17 mg/kg; Molecular Probes, Eugene, OR) was administered IA 5 minutes after induction of ischemia. To assess the microvascular distribution of fibrin(ogen), 3 to 5 postcapillary venules in the cremaster muscle or 5 high power fields of sinusoids in the liver were randomly analyzed in WT and PAI-1-deficient animals undergoing I/R (30/90-minute ischemia and 120-minute reperfusion; n=3 per group). Deposition of Alexa 488-conjugated fibrin(ogen) was analyzed by measuring fluorescence intensity profiles using Image J software (National Institutes of Health).

(Immuno)histochemistry

To determine the phenotype of transmigrated leukocytes, immunostaining of paraffin-embedded serial tissue sections of the cremaster muscle or the liver was performed. Sections were incubated with primary rat antimouse anti-Ly-6G, anti-CD45 (BD Biosciences), anti-F4/80 (Serotec, Oxford, UK) IgG, or isotype control antibodies. Afterwards, the paraffin sections were stained with commercially available immunohistochemistry kits (Ly-6G, CD45, Super Sensitive Link-Label IHC detection system; BioGenex, San Ramon, CA; F4/80, Vectastain ABC kit, Vector Laboratories, Burlingame, CA), obtaining an easily detectable reddish or brownish end product, respectively, or fluorescence-labeled secondary antibodies. Finally, the sections were counterstained with Mayer hemalaun. The number of extravascularly localized Ly-6G-, CD45-, or F4/80-positive cells was quantified by light microscopy (magnification \times 400) on 3 sections (10 observation fields per section) from 6 individual animals per experimental group in a blinded manner. The number of

transmigrated Ly-6G-positive cells (neutrophils) and F4/80-positive cells (monocytes/macrophages) is expressed as the percentage of total CD45-positive leukocytes.

Paraffin-embedded liver sections were also stained by terminal deoxynucleotidyl transferase-mediated deoxyuridine triphosphate-digoxenin nick-end labeling (TUNEL) using a commercially available kit (Roche-Boehringer Mannheim, Co, Germany). TUNEL-positive cells were counted in a blinded manner using light microscopy (magnification 400 \times) in 10 high power fields.

Confocal Microscopy

For the analysis of PAI-1 deposition, cremaster muscles were prepared as described previously.⁹ After incubation with an anti-Ly6G antibody (Invitrogen, Carlsbad, CA), an Alexa Fluor 647 anti-CD31 monoclonal antibody (Invitrogen), and a rabbit anti-mouse anti-PAI-1 antibody (Abcam, Cambridge, UK), tissues were incubated with the secondary Alexa Fluor 488-linked goat antirat or Alexa Fluor 546-linked goat antirabbit antibody (Invitrogen). Immunostained tissues were mounted in PermaFluor (Beckman Coulter, Fullerton, CA) on glass slides and observed using a Leica SP5 confocal laser-scanning microscope (Leica Microsystems, Wetzlar, Germany).

Liver Enzymes

Whole-blood samples were collected via cardiac puncture at the end of the experiment and immediately centrifuged at 2000g for 10 minutes. Supernatant plasma was retrieved and stored at -80°C . Serum AST and ALT activities were determined at 37°C with an automated analyzer (Hitachi 917; Roche-Boehringer, Mannheim, Germany) using standardized test systems (HiCo GOT and HiCo GPT; Roche-Boehringer).

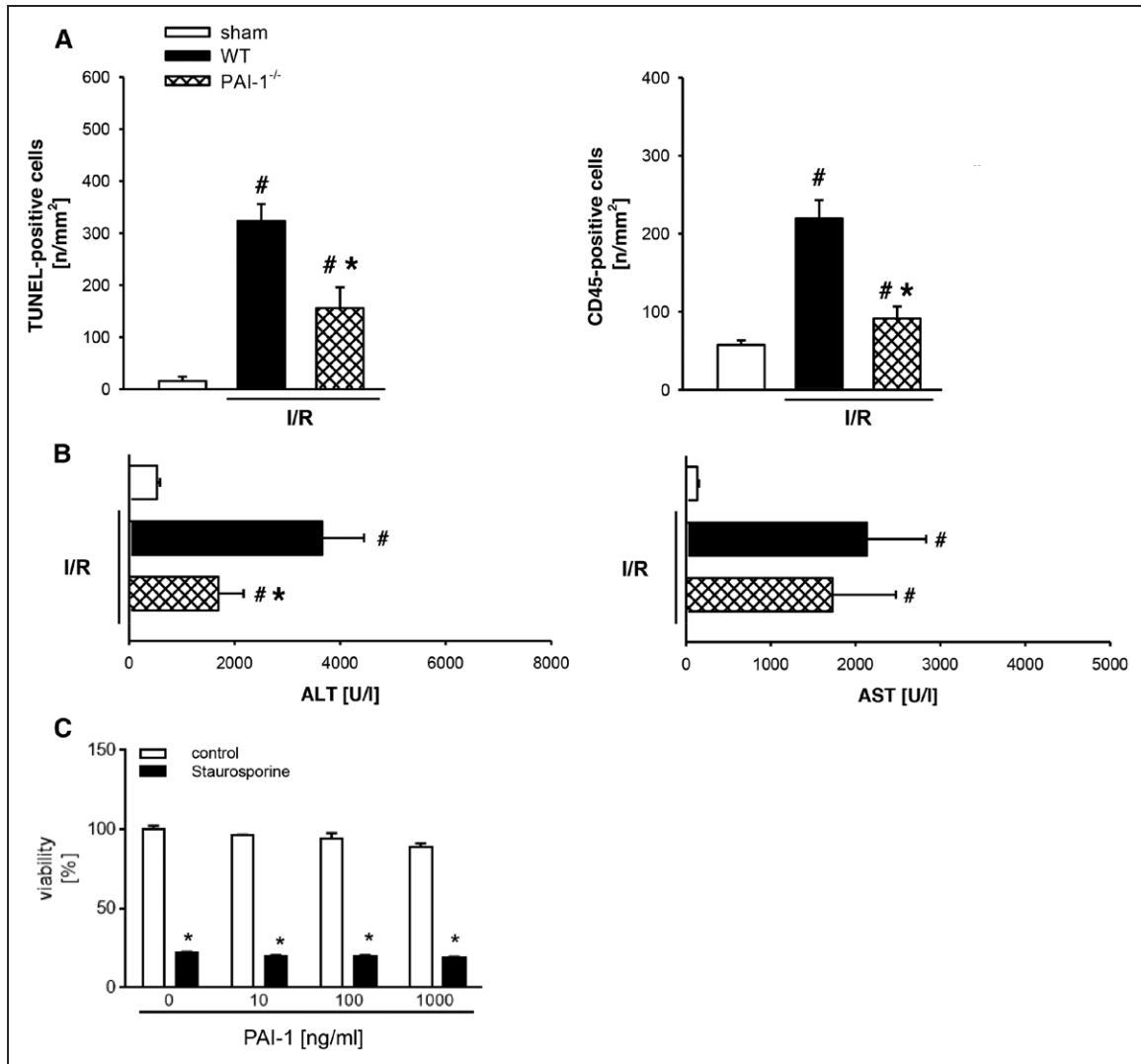


Figure 5. Role of plasminogen activator inhibitor-1 (PAI-1) for hepatic ischemia-reperfusion (I/R) injury. In a model of warm hepatic I/R (90/120 min) injury, the number of apoptotic/necrotic (TUNEL [terminal deoxynucleotidyl transferase dUTP nick-end labeling]-positive) hepatocytes and the recruitment of CD45-positive leukocytes to the postischemic liver were analyzed as detailed in Material and Methods in the [online-only Data Supplement](#). Panels show quantitative data for TUNEL- or CD45-positive cells (**A**) and for serum levels of glutamate-pyruvate transaminase/alanine transaminase (ALT) or glutamate-oxalacetate transaminase/aspartate aminotransferase (AST; **B**) in sham-operated wild-type (WT) mice as well as WT and PAI-1-deficient mice (mean±SEM for n=6 per group; [#]*P*<0.05, vs sham; ^{*}*P*<0.05, vs WT). Cell death of primary hepatocytes isolated from WT mice was analyzed by Alamar Blue reduction assays as detailed in Material and Methods in the [online-only Data Supplement](#). **C**, Quantitative data for hepatocytes exposed to varying doses of recombinant murine PAI-1, staurosporine (used as a positive control death stimulus), or vehicle (mean±SEM for n=3 per group; [#]*P*<0.05, vs control).

Viability of Hepatocytes

Potential direct cytotoxic or cytoprotective effects of PAI-1 were determined by Alamar Blue reduction assays with primary murine hepatocytes as described previously.²² Briefly, hepatocytes were isolated from C57BL/6 mice by liver perfusion and percoll density centrifugation and seeded into gelatin-coated multiwell plates in William E complete medium supplemented with 50 ng/mL epidermal growth factor, 1 μg/mL insulin, 10 μg/mL transferrin, and 1.3 μg/mL hydrocortisone (all from Sigma-Aldrich, Taufkirchen, Germany). Adhesion was allowed overnight, and cells were exposed to 0 to 1000 ng/mL PAI-1 for 24 hours. Ten micromoles per liter Staurosporine (Sigma-Aldrich) served as positive control death stimulus. Subsequently, the medium was aspirated, cells were washed, and Alamar Blue reagent was added. Metabolic resazurin reduction was allowed for 10 hours, and resorufin fluorescence was determined with a Synergy Mx microplate reader (BioTek, Bad Friedrichshall, Germany). Primary

fluorescence data were calibrated on the untreated controls (100% viability).

Flow Cytometry

To evaluate the effect of PAI-1 on the binding of intercellular adhesion molecule-1 (ICAM-1)/CD54 to primary mouse neutrophils, anticoagulated whole-blood samples of WT mice were suspended in Hanks balanced salt solution containing 1 mmol/L CaCl₂ and MgCl₂ (Life Technologies, Carlsbad, CA) and incubated (for 5 minutes at 37°C) with different concentrations (1–100 ng/mL) of PAI-1 or phorbol myristate acetate (1 ng/mL) as a positive control and with PBS, in the presence of ICAM-1/Fc (10 μg/mL; R&D Systems), VCAM-1/fragment crystallizable (Fc; 10 μg/mL; R&D Systems), and phycoerythrin-conjugated antihuman IgG1 (Fc-specific; Southern Biotechnology). In further experiments, cells were treated with a RAP or vehicle, anti-LRP-1 antibody or isotype control antibody, SB203580 (25 μmol/L; Sigma Aldrich),

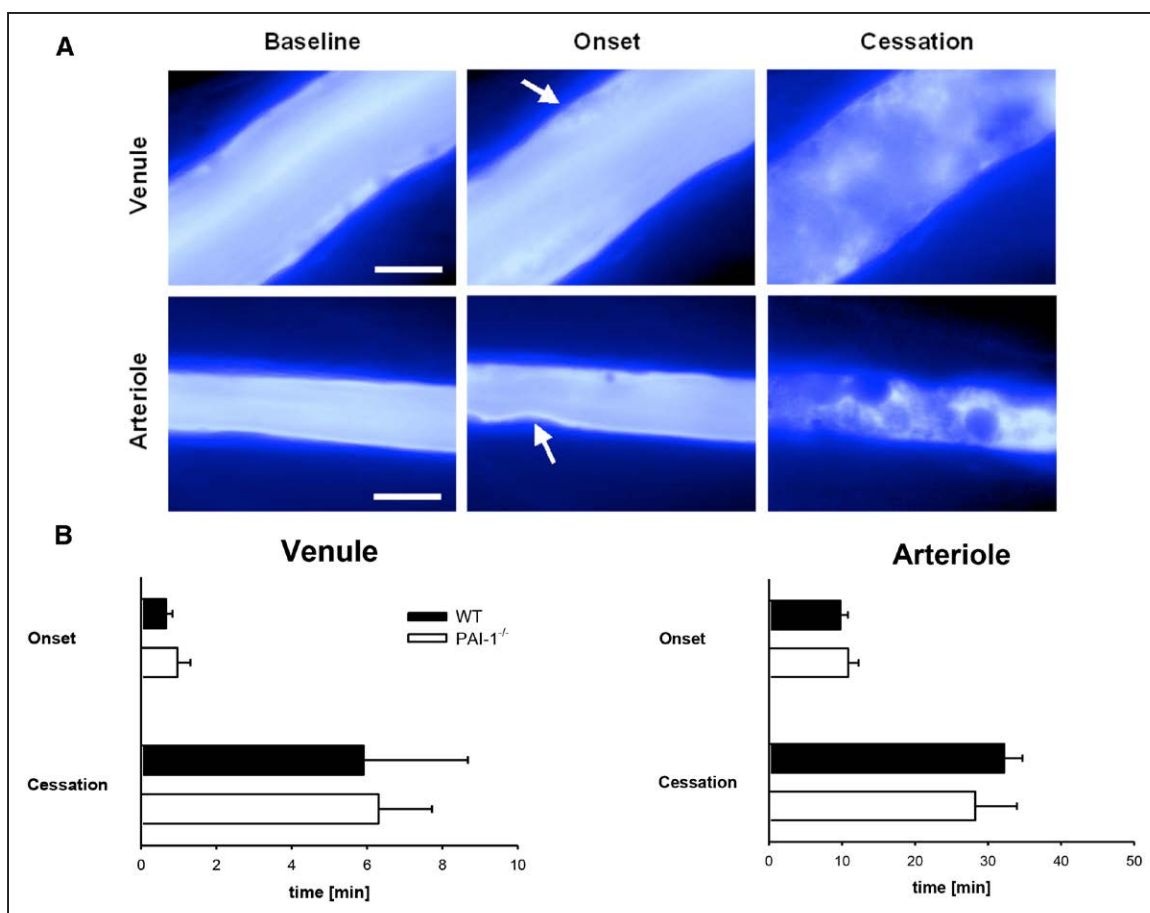


Figure 6. Role of plasminogen activator inhibitor-1 (PAI-1) for microvascular thrombus formation. Thrombus formation in microvessels of the cremaster muscle of wild-type (WT) mice was induced by phototoxic injury and analyzed by fluorescence *in vivo* microscopy as detailed in Material and Methods in the [online-only Data Supplement](#), representative images are shown (**A**). Panels show quantitative data for the onset of thrombus formation and the cessation of blood flow in venules and arterioles of WT and PAI-1-deficient mice (**B**; mean±SEM for n=4 per group).

SP600125 (5 $\mu\text{mol/L}$; Sigma Aldrich), FR180204 (15 $\mu\text{mol/L}$; Sigma Aldrich) or vehicle. After washing, cells were labeled with antibodies directed against CD45, CD11b, CD115, and Gr1. Binding of ICAM-1/CD54 or VCAM-1/CD106 was measured by a flow cytometer (Gallios, Beckmann Coulter). In separate experiments, expression of PAI-1 and LRP-1 was analyzed in neutrophils isolated from the peripheral blood of WT mice or in HMECS using anti-PAI-1 or LRP-1 antibodies (see above). The results were analyzed with FlowJo Software (Treestar).

Statistics

All *in vivo* experiments and data analyses were performed in a blinded manner.

Data analysis was performed with a statistical software package (SigmaStat for Windows; Jandel Scientific, Erkrath, Germany). After testing normality of data (using the Shapiro–Wilk test), the 1-way ANOVA test followed by the Student–Newman–Keuls test (>2 groups) or the *t* test (2 groups) was used for the estimation of stochastic probability in intergroup comparisons. Mean values and SEM are given. *P* values <0.05 were considered significant.

Results

Role of PAI-1 for Postischemic Leukocyte Responses

To understand the role of PAI-1 in I/R injury, we first characterized the distribution of PAI-1 in postischemic tissue by immunostaining of whole mounts of the mouse

cremaster muscle and confocal laser scanning microscopy analyses (Figure 1A). In response to I/R, PAI-1 was primarily found on the surface of PECAM-1 (platelet endothelial cell adhesion molecule-1)/CD31⁺ venular endothelial cells and on Ly-6G⁺ neutrophils as well as extravasated into the perivascular tissue, whereas it was barely detected in cremasteric microvessels of sham-operated animals. In line with these results, expression of PAI-1 was low in neutrophils isolated from the peripheral blood of wild-type (WT) mice as well as in unstimulated microvascular endothelial cells as assessed by flow cytometry (Figure I in the [online-only Data Supplement](#)). On activation with tumor necrosis factor, in contrast, PAI-1 expression was significantly increased in these cells. Furthermore, expression of the PAI-1 receptor LRP-1 (low-density lipoprotein receptor–related protein-1) was significantly elevated on stimulation with tumor necrosis factor in neutrophils and endothelial cells (Figure II in the [online-only Data Supplement](#)). However, postischemic microvascular PAI-1 presentation was not affected by neutrophil depletion or antibody blockade of LRP-1 (Figure III in the [online-only Data Supplement](#)).

Leukocyte recruitment to postischemic tissue is a hallmark of I/R injury.^{1,2} To characterize the functional relevance of

PAI-1 for the single steps of the extravasation process of neutrophils to postischemic tissue, we used near-infrared reflected light oblique transillumination *in vivo* microscopy in the cremaster muscle of WT and PAI-1-deficient mice (Figure 1B). As well-known, surgical preparation of the cremaster muscle induced leukocyte rolling in postcapillary venules. After 30 minutes of ischemia and 60 minutes of reperfusion, there was a significant increase in numbers of rolling leukocytes as compared with sham-operated animals that returned to baseline values after 120 minutes of reperfusion. PAI-1 deficiency did not significantly alter leukocyte rolling during the entire reperfusion phase (data not shown). Under baseline conditions before I/R, few leukocytes were found firmly adherent to the vessel wall of postcapillary venules. In contrast, after 30 minutes of ischemia and 120 minutes of reperfusion, there was a significant elevation in numbers of firmly adherent leukocytes as compared with sham-operated controls. This elevation was significantly reduced in PAI-1-deficient animals. Before I/R, only few transmigrated leukocytes were detected within the perivascular tissue. In response to I/R, the number of transmigrated leukocytes was significantly increased as compared with sham-operated controls. Similar to our results for leukocyte firm adherence, the postischemic increase in leukocyte transmigration was significantly attenuated in PAI-1-deficient mice (Figure 1B).

To characterize the functional relevance of leukocyte versus nonleukocyte PAI-1 for postischemic leukocyte responses, we performed cell transfer experiments (Figure 1C). In postcapillary venules of the postischemic cremaster muscle, the numbers of adherent and transmigrated WT donor leukocytes were significantly diminished in PAI-1-deficient recipient mice as compared with WT mice receiving cells from WT donors. Similarly, the numbers of adherent and transmigrated cells of PAI-1-deficient donors were significantly lower in WT recipients.

As a corollary to the experiments on PAI-1^{-/-} mice, we also measured the effects of exogenously applied PAI-1. For this purpose, varying doses of murine PAI-1 were directly injected into the scrotum of WT mice. After 240 minutes of exposure to PAI-1, there was a dose-dependent increase in numbers of firmly adherent and transmigrated leukocytes as compared with PBS-treated controls, whereas leukocyte rolling was not significantly altered (Figure 2A). Furthermore, no significant differences were detected in numbers of intravascularly rolling and firmly adherent as well as transmigrated leukocytes between animals receiving an intrascrotal injection of active PAI-1 or latent (inactive) PAI-1 lacking antifibrinolytic activity (Figure IV in the [online-only Data Supplement](#)).

Phenotyping Transmigrated Leukocytes

To identify the phenotype of transmigrated leukocytes, immunostaining for CD45 (common leukocyte antigen), Ly-6G (neutrophils), and F4/80 (monocytes/macrophages) of cremasteric tissue samples was performed. In response to I/R and on intrascrotal injection of PAI-1, >85% of transmigrated leukocytes were positive for Ly-6G and ≈15% of transmigrated leukocytes were positive for F4/80.

Microhemodynamic Parameters and Systemic Leukocyte Counts

To assure intergroup comparability in our *in vivo* microscopy analyses, quantification of inner vessel diameters, blood flow velocities, and wall shear rates of analyzed postcapillary venules, as well as systemic leukocyte counts, was performed (Table I in the [online-only Data Supplement](#)). No significant differences were detected among all experimental groups.

Role of LRP-1 for PAI-1-Dependent Leukocyte Responses

Previous studies have documented that PAI-1 is capable of interacting with LRP-1 which is also known as α -2-macroglobulin receptor, apolipoprotein E receptor, or CD91.²³⁻²⁵ To analyze the functional relevance of LRP-1 for postischemic leukocyte responses, we performed an additional set of experiments. Application of RAP (receptor-associated protein), an inhibitor of LRP-1 and other members of the low-density lipoprotein receptor family, or antibodies specifically directed against LRP-1 significantly reduced postischemic intravascular adherence and transmigration of leukocytes to postischemic tissue (Figure VA in the [online-only Data Supplement](#)) but did not significantly alter intravascular leukocyte rolling (data not shown). In line with these results, application of the LRP-1 inhibitor RAP or blocking antibodies directed against LRP-1 almost completely abolished PAI-1-elicited intravascular adherence and transmigration of neutrophils (Figure 2B and 2C). Because specific inhibition of LRP-1 achieved >50% of the inhibitory effect of RAP, our data suggest that LRP-1 serves as the principal receptor of the low-density lipoprotein receptor family for PAI-1-dependent leukocyte responses. Moreover, PAI-1-dependent intravascular adherence of leukocytes was nearly abrogated on antibody blockade of the β 2 integrins Mac-1/CD11b or (to a lesser degree) of LFA-1 (lymphocyte function-associated antigen-1)/CD11a, whereas leukocyte transmigration to the perivascular tissue was significantly reduced on antibody blockade of Mac-1/CD11b but not of LFA-1/CD11a (Figure 2D).

Effect of PAI-1 on Activation of Neutrophils and Endothelial Cells

Intravascular adherence and the subsequent transmigration of leukocytes to the perivascular tissue require interactions of leukocyte integrins in higher affinity conformation and their endothelial binding partners, such as intercellular adhesion molecule (ICAM)-1/CD54 or vascular cell adhesion molecule (VCAM)-1/CD106.²⁶⁻²⁹ Because PAI-1-elicited intravascular adherence of neutrophils was strictly dependent on β 2 integrins (see above), we hypothesized that PAI-1 induces affinity changes in neutrophil β 2 integrins.

As a measure of conformational changes of β 2 integrins, binding of ICAM-1/CD54 (which predominantly interacts with β 2 integrins) to neutrophils (CD45⁺ CD11b⁺ Gr-1⁺ CD115⁻ cells) isolated from the peripheral blood of WT mice was analyzed by multichannel flow cytometry (Figure 3A). We found that the direct stimulation with PAI-1 induced a significant increase in the binding of ICAM-1/CD54 to neutrophils as compared with PBS-treated controls whereas surface expression levels of β 2 integrins/CD18 on neutrophils as well

as the binding of VCAM-1/CD106 (which interacts with β 1 integrins) to neutrophils remained unaltered. This increase in ICAM-1/CD54 binding was significantly reduced on application of the LRP-1 inhibitor RAP, of blocking antibodies directed against LRP-1, or of inhibitors of p38, extracellular signal-regulated kinases 1 and 2, and c-Jun N-terminal kinases mitogen-activated protein kinases (MAPK; Figure 3B and 3C). Importantly, exposure to MAPK inhibitors or blocking anti-LRP-1 antibodies did not significantly alter ICAM-1/CD54 binding to unstimulated neutrophils (Figure VI in the [online-only Data Supplement](#)). Similarly, no significant differences were detected in CD18 expression or the binding capacity for ICAM-1/CD54 or VCAM-1/CD106 between WT and PAI-1-deficient neutrophils undergoing exposure to PAI-1 (Figure VII in the [online-only Data Supplement](#)).

In contrast to these results, exposure to PAI-1 did not significantly alter expression levels of ICAM-1/CD54 or VCAM-1/CD106 on microvascular endothelial cells (Figure VIII in the [online-only Data Supplement](#)).

Role of PAI-1 in Postischemic Microvascular Leakage

In addition to neutrophil infiltration, microvascular leakage is a key event in the pathogenesis of I/R injury that leads to loss of intravascular fluid and causes interstitial edema ultimately compromising proper reperfusion of postischemic tissue.^{1,2} The role of PAI-1 for the control of microvascular permeability during I/R is still unclear. As a measure of microvascular permeability, leakage of high molecular weight fluorescein isothiocyanate dextran to the postischemic cremaster muscle was analyzed by *in vivo* fluorescence microscopy (Figure 4A). After 30 minutes of ischemia and 150 minutes of reperfusion, there was a significant increase in the leakage of fluorescein isothiocyanate dextran in WT mice as compared with sham-operated controls. This increase was significantly diminished in PAI-1-deficient mice and in WT mice treated with blocking anti-LRP-1 antibodies (Figure 4A; Figure VB in the [online-only Data Supplement](#)).

In a further set of experiments, we sought to evaluate the mechanisms underlying the effect of PAI-1 on microvascular barrier function in more detail. Intrascrotal injection of PAI-1 lead to a significant increase in the leakage of fluorescein isothiocyanate dextran as compared with unstimulated controls. This increase was almost completely abolished in animals depleted from neutrophils. *In vitro*, exposure of confluent HMEC (human microvascular endothelial cell line-1) endothelial cell layers to PAI-1 induced a dose-dependent reduction in macromolecular permeability which was not significantly altered on application of the LRP-1 inhibitor RAP (Figure 4B).

Role of PAI-1 in Warm Hepatic I/R Injury

To transfer these findings into a clinically relevant situation, the role of PAI-1 was analyzed in a model of warm hepatic I/R injury. As a measure of cell death, the number of TUNEL (terminal deoxynucleotidyl transferase dUTP nick-end labeling)-positive cells was quantified in hepatic tissue sections. In the liver of sham-operated control mice, only few TUNEL-positive cells were detected. In contrast, the number of TUNEL-positive cells was significantly elevated on I/R.

This elevation was significantly diminished in PAI-1-deficient mice (Figure 5A). In sham-operated animals, the number of leukocytes in the perivascular tissue was found to be low. After 90 minutes of ischemia and 120 minutes of reperfusion, however, there was a significant increase in numbers of neutrophils (>70% Ly-6G-positive leukocytes) transmigrated to the liver. This increase was significantly reduced in PAI-1-deficient mice (Figure 5A). In addition, serum levels of transaminases were determined in our experiments as a further measure of tissue injury. After 90 minutes of ischemia and 120 minutes of reperfusion, there was a significant increase in serum levels of aspartate aminotransferase and alanine transaminase as compared with sham-operated controls. In line with our concept, PAI-1 deficiency significantly attenuated serum levels of alanine transaminase and slightly those of aspartate aminotransferase; however, the decrease of aspartate aminotransferase did not reach statistical significance (Figure 5B).

In vitro, exposure to PAI-1 did not directly affect the viability of primary hepatocytes isolated from WT mice whereas the indol alkaloid staurosporine significantly reduced the viability of these cells in a dose-dependent manner (Figure 5C).

Role of PAI-1 for Microvascular Thrombus Formation

With regard to its well-known inhibitory action on plasminogen activators, deficiency of PAI-1 might exhibit hyperfibrinolytic effects, thereby interfering with microvascular hemostasis potentially causing microvascular hemorrhage. Using a model of phototoxic injury-induced thrombus formation in cremasteric microvessels, the role of PAI-1 for microvascular thrombogenesis was evaluated (Figure 6A). We found that onset and cessation times in arterioles and venules of PAI-1-deficient mice did not significantly differ from those in WT mice (Figure 6B).

To assure intergroup comparability, fluorescence intensity levels, systemic leukocyte counts, and microhemodynamic parameters were measured in all experiments. No significant differences were observed among the experimental groups (Table II in the [online-only Data Supplement](#)).

Moreover, postischemic deposition of Alexa488-conjugated fibrin(ogen) in cremasteric postcapillary venules (Figure IXA in the [online-only Data Supplement](#)) or hepatic sinusoids (Figure IXB in the [online-only Data Supplement](#)) did not significantly vary between WT and PAI-1-deficient mice.

Effect of TM5275 on Postischemic Leukocyte Responses and Liver Injury

In an additional set of experiments, we tested the effect of the PAI-1 inhibitor TM5275 on postischemic leukocyte responses. Application of this compound 5 minutes before reperfusion significantly reduced intravascular adherence and (subsequent) transmigration of neutrophils to the perivascular tissue in the cremaster muscle of WT mice undergoing 30 minutes of ischemia and 120 minutes of reperfusion as compared with vehicle treated control animals but did not significantly change leukocyte rolling (Figure X in the [online-only Data Supplement](#)). In contrast, the number of Ly-6G-positive neutrophils recruited to the reperfused liver as well as postischemic serum levels of aspartate aminotransferase and alanine transaminase were

only slightly but not significantly altered on application of TM5275 (Figure XI in the [online-only Data Supplement](#)).

Discussion

PAI-1 is increasingly recognized as modulator of nonfibrinolytic processes,^{4,13} including I/R injury.^{30–35} The underlying mechanisms remain poorly understood. In the postischemic inflammatory response, leukocytes accumulate in the microvasculature and infiltrate the perivascular tissue, thereby compromising proper reperfusion and amplifying the ischemic tissue injury.^{1,2} To characterize the contribution of PAI-1 to these events, we used different *in vivo* and *ex vivo* microscopy techniques in genetically modified mice. In I/R injury, PAI-1 was found to be presented on the endothelium of postcapillary venules as well as on infiltrating neutrophils. Together with circulating PAI-1, this protease inhibitor is thought to bind to cell surface glycosaminoglycans which enhances its biological activity.^{36,37} As a consequence of this process, PAI-1 derived from both leukocytes and nonleukocytic sources promoted postischemic neutrophil adherence to the microvascular endothelium and supported the subsequent transmigration of these immune cells to the interstitial tissue. Our findings extend previous observations in which blockade of PAI-1 was associated with reduced leukocyte infiltration of the reperfused tissue on postischemic lung injury.³²

Beyond its inhibitory effects on the plasminogen activators tPA and urokinase-type plasminogen activator, PAI-1 interacts with LRP-1, a member of the low-density lipoprotein receptor family, which serves as a multifunctional scavenger and signaling receptor in various biological processes,^{23–25} including leukocyte trafficking.³⁸ Because LRP-1 is expressed on the surface of neutrophils, we hypothesized that PAI-1 mediates postischemic neutrophil responses via this receptor protein. In our experiments, we show that blockade of LRP-1 significantly diminishes intravascular adherence and subsequent transmigration of neutrophils to postischemic tissue. Moreover, we found that exogenously administered, recombinant PAI-1 is capable of inducing neutrophil responses, which were strictly dependent on LRP-1. In this context, we did not detect any differences on the capability to elicit neutrophil extravasation between active PAI-1 and latent PAI-1 lacking antifibrinolytic activity indicating that this protease inhibitor recruits neutrophils independently of its well-known antifibrinolytic properties. Thus, our data suggest that endothelially presented PAI-1 acts as an inflammatory mediator that directs circulating neutrophils to postischemic tissue by engaging LRP-1.

Toward a more comprehensive, mechanistic understanding of these processes, we sought to elaborate the molecular basis underlying PAI-1-dependent neutrophil responses in further experiments. Leukocyte adherence to microvascular endothelial cells is facilitated by interactions of leukocyte integrins with their endothelial binding partners of the immunoglobulin superfamily (eg, ICAM-1/CD54, VCAM-1/CD106). This process requires the induction of higher affinity conformations of leukocyte integrins typically elicited by endothelially presented chemokines or other inflammatory mediators.^{26–29} Consequently, endothelially presented PAI-1 might initiate conformational changes in neutrophil integrins to regulate postischemic neutrophil responses. In line with

this concept, we document that PAI-1 induces higher affinity conformations of $\beta 2$ integrins in neutrophils but does not activate microvascular endothelial cells. These events were found to require LRP-1 and MAPK-dependent signaling pathways. Moreover, we show that PAI-1-dependent adherence of neutrophils to the microvascular endothelium (but not intravascular rolling) is mediated by the $\beta 2$ integrins LFA-1/CD11a and Mac-1/CD11b. In summary, these results indicate that PAI-1 promotes neutrophil trafficking to postischemic tissue through interaction with LRP-1 in intravascularly rolling neutrophils which, in turn, induces conformational changes of neutrophil $\beta 2$ integrins via MAPK-dependent signaling pathways.

In addition to leukocyte recruitment, endothelial dysfunction and enhanced microvascular permeability represent key factors of I/R injury.^{1,2} With respect to previous reports documenting the participation of PAI-1 in the regulation of vascular permeability during cardiac fibrosis³⁹ and ischemic brain injury,³³ we hypothesized that PAI-1 is involved in the control of postischemic microvascular leakage. Here, we demonstrate that PAI-1 deficiency or blockade of its receptor LRP-1 potentially protect the microvasculature from its postischemic loss of barrier function. Conversely, we found that exogenous administration of recombinant PAI-1 induced a significant elevation in microvascular permeability. Importantly, neutrophil depletion completely abolished PAI-1-elicited microvascular leakage *in vivo* whereas addition of recombinant PAI-1 to microvascular endothelial cell layers *in vitro* even reduced their macromolecular permeability in an LRP-1-independent manner. Our findings, therefore, suggest that PAI-1 promotes postischemic microvascular leakage indirectly through the recruitment of neutrophils but does not directly affect microvascular integrity. In this context, it has previously been reported that intravascularly adherent neutrophils increase microvascular permeability through secreted products (eg, chemokines/cytokines or reactive oxygen species) as well as via adhesion-dependent processes involving $\beta 2$ integrins and endothelial ICAM-1/CD54.⁴⁰

To transfer these findings into a clinically more relevant situation, we used a hepatic I/R injury model. In our experiments, deficiency of PAI-1 significantly diminished neutrophil infiltration of the postischemic liver. These effects were associated with a strong attenuation of hepatic I/R injury as indicated by reduced numbers of apoptotic/necrotic hepatocytes and decreased serum levels of transaminases. Because PAI-1 did not exhibit direct cytotoxic or cytoprotective effects on primary hepatocytes *in vitro*, our results suggest that the immediate specific and effective blockade of PAI-1 in the acute inflammatory response on I/R protects from postischemic liver injury via inhibition of neutrophil-mediated cell death. Noteworthy, however, prolonged blockade (genetic deficiency) of PAI-1 resulted in accelerated myocardial rupture,⁴¹ enhanced cardiac fibrosis,⁴² and increased inflammatory cell influx³⁵ on experimental myocardial infarction. In contrast, pharmacological inhibition of PAI-1 showed no effect on postischemic liver injury or cardiac remodeling,³⁴ whereas—in line with our results—deficiency of this serpin was associated with reduced tissue injury early on I/R of the lung.³² Similarly, in acute cerebral I/R, administration of an inhibitor directed against PAI-1 and thrombin activatable fibrinolysis

inhibitor led to mitigated brain damage and improved functional outcomes.^{30,31} Hence, the appropriate timing for effective interference with the action of PAI-1 seems to be critical for its successful application in the treatment of I/R injury.

Manipulating the fibrinolytic system might not only cause side effects on tissue remodeling (because of the modulation of plasmin-dependent activation of matrix metalloproteinases) but might also lead to enhanced thrombus formation (as a consequence of reduced fibrinolysis)^{43–47} or to hematoma formation (as a result of exaggerated fibrinolysis).⁴⁸ All these conditions might compromise postischemic organ function. Recent observations, however, indicate that pharmacological blockade of PAI-1 results in a prominent profibrinolytic effect without increased bleeding from larger vessels.³¹ Because leukocytes are critically involved in thrombus formation in larger vessels,^{49,50} these effects might not only be explained by hyperfibrinolysis but also be because of a reduction of leukocyte-mediated prothrombotic effects in this particular pathological context. To evaluate the role of PAI-1 in microvascular hemostasis, we used a model of thrombosis elicited by photochemical injury. In these experiments, we were able to demonstrate that deficiency of PAI-1 does not alter thrombogenesis in the microvasculature. Moreover, PAI-1 deficiency was not associated with increased deposition of fibrin(ogen) on the postischemic microvascular endothelium. Consequently, these data indicate that the immediate interference with PAI-1 might provide a safe strategy for the prevention and treatment of early I/R injury.

In conclusion, our experimental findings identify a previously unrecognized function of PAI-1 as an inflammatory mediator that is rapidly deposited on the microvascular endothelium on I/R and subsequently induces conformational changes in $\beta 2$ integrins of intravascularly rolling neutrophils. These events are mediated through LRP-1 and MAPK-dependent signaling pathways that, in turn, promote accumulation of neutrophils in the reperfused tissue. During this process, neutrophils disrupt endothelial junctions and support the postischemic microvascular leakage. Conversely, deficiency of PAI-1 effectively attenuated neutrophil recruitment, microvascular dysfunction, and tissue injury on experimental I/R without exhibiting side effects on microvascular hemostasis. Our findings provide novel insights into the non-fibrinolytic functions of the fibrinolytic system and suggest the blockade of PAI-1 (eg, by angiotensin-converting enzyme inhibitors lowering serum levels of PAI-1^{51,52} or specific and effective PAI-1 inhibitors) as a promising strategy for the prevention and treatment of I/R injury.

Acknowledgments

We thank Alke Schropp and Gerhard Adams for technical assistance. This study is part of the doctoral thesis of M. Fabritius.

Sources of Funding

This study was supported by Deutsche Forschungsgemeinschaft (DFG; SFB 914 to F. Krombach and C.A. Reichel [project B3] and K. Lauber [project B6]).

Disclosures

None.

References

- Eltzschig HK, Eckle T. Ischemia and reperfusion—from mechanism to translation. *Nat Med*. 2011;17:1391–1401. doi: 10.1038/nm.2507.
- Schofield ZV, Woodruff TM, Halai R, Wu MC, Cooper MA. Neutrophils—a key component of ischemia-reperfusion injury. *Shock*. 2013;40:463–470. doi: 10.1097/SHK.0000000000000044.
- Gasser O, Schifferli JA. Activated polymorphonuclear neutrophils disseminate anti-inflammatory microparticles by ectocytosis. *Blood*. 2004;104:2543–2548. doi: 10.1182/blood-2004-01-0361.
- Syrovets T, Lunov O, Simmet T. Plasmin as a proinflammatory cell activator. *J Leukoc Biol*. 2012;92:509–519. doi: 10.1189/jlb.0212056.
- Smith HW, Marshall CJ. Regulation of cell signalling by uPAR. *Nat Rev Mol Cell Biol*. 2010;11:23–36. doi: 10.1038/nrm2821.
- Del Rosso M, Margheri F, Serrati S, Chillà A, Laurenzana A, Fibbi G. The urokinase receptor system, a key regulator at the intersection between inflammation, immunity, and coagulation. *Curr Pharm Des*. 2011;17:1924–1943.
- Reichel CA, Kanse SM, Krombach F. At the interface of fibrinolysis and inflammation: the role of urokinase-type plasminogen activator in the leukocyte extravasation cascade. *Trends Cardiovasc Med*. 2012;22:192–196. doi: 10.1016/j.tcm.2012.07.019.
- Reichel CA, Lerchenberger M, Uhl B, Rehberg M, Berberich N, Zahler S, Wymann MP, Krombach F. Plasmin inhibitors prevent leukocyte accumulation and remodeling events in the postischemic microvasculature. *PLoS One*. 2011;6:e17229. doi: 10.1371/journal.pone.0017229.
- Reichel CA, Uhl B, Lerchenberger M, Pühr-Westerheide D, Rehberg M, Liebl J, Khandoga A, Schmalix W, Zahler S, Deindl E, Lorenzl S, Declercq PJ, Kanse S, Krombach F. Urokinase-type plasminogen activator promotes paracellular transmigration of neutrophils via Mac-1, but independently of urokinase-type plasminogen activator receptor. *Circulation*. 2011;124:1848–1859. doi: 10.1161/CIRCULATIONAHA.110.017012.
- Uhl B, Zuchtriegel G, Pühr-Westerheide D, Praetner M, Rehberg M, Fabritius M, Hessenauer M, Holzer M, Khandoga A, Fürst R, Zahler S, Krombach F, Reichel CA. Tissue plasminogen activator promotes post-ischemic neutrophil recruitment via its proteolytic and nonproteolytic properties. *Arterioscler Thromb Vasc Biol*. 2014;34:1495–1504. doi: 10.1161/ATVBAHA.114.303721.
- Lerchenberger M, Uhl B, Stark K, Zuchtriegel G, Eckart A, Miller M, Pühr-Westerheide D, Praetner M, Rehberg M, Khandoga AG, Lauber K, Massberg S, Krombach F, Reichel CA. Matrix metalloproteinases modulate ameiboid-like migration of neutrophils through inflamed interstitial tissue. *Blood*. 2013;122:770–780. doi: 10.1182/blood-2012-12-472944.
- Czekay RP, Wilkins-Port CE, Higgins SP, Freytag J, Overstreet JM, Klein RM, Higgins CE, Samarakoon R, Higgins PJ. PAI-1: an integrator of cell signaling and migration. *Int J Cell Biol*. 2011;2011:562481. doi: 10.1155/2011/562481.
- Declercq PJ, Gils A. Three decades of research on plasminogen activator inhibitor-1: a multifaceted serpin. *Semin Thromb Hemost*. 2013;39:356–364. doi: 10.1055/s-0033-1334487.
- Meade TW, Ruddock V, Stirling Y, Chakrabarti R, Miller GJ. Fibrinolytic activity, clotting factors, and long-term incidence of ischaemic heart disease in the Northwick Park Heart Study. *Lancet*. 1993;342:1076–1079.
- Van Dreden P, Rousseau A, Savoure A, Lenormand B, Fontaine S, Vasse M. Plasma thrombomodulin activity, tissue factor activity and high levels of circulating procoagulant phospholipid as prognostic factors for acute myocardial infarction. *Blood Coagul Fibrinolysis*. 2009;20:635–641. doi: 10.1097/MBC.0b013e32832e05dd.
- Vaughan DE. PAI-1 and atherothrombosis. *J Thromb Haemost*. 2005;3:1879–1883. doi: 10.1111/j.1538-7836.2005.01420.x.
- Wiman B, Andersson T, Hallqvist J, Reuterwall C, Ahlbom A, deFaire U. Plasma levels of tissue plasminogen activator/plasminogen activator inhibitor-1 complex and von Willebrand factor are significant risk markers for recurrent myocardial infarction in the Stockholm Heart Epidemiology Program (SHEEP) study. *Arterioscler Thromb Vasc Biol*. 2000;20:2019–2023.
- Baez S. An open cremaster muscle preparation for the study of blood vessels by in vivo microscopy. *Microvasc Res*. 1973;5:384–394.
- Mempel TR, Moser C, Hutter J, Kuebler WM, Krombach F. Visualization of leukocyte transendothelial and interstitial migration using reflected light oblique transillumination in intravital video microscopy. *J Vasc Res*. 2003;40:435–441.
- Ades EW, Candal FJ, Swerlick RA, George VG, Summers S, Bosse DC, Lawley TJ. Hmec-1: establishment of an immortalized human microvascular endothelial cell line. *J Invest Derm*. 1992;99:683–690.
- Bihari P, Holzer M, Praetner M, Fent J, Lerchenberger M, Reichel CA, Rehberg M, Lakatos S, Krombach F. Single-walled carbon nanotubes

- activate platelets and accelerate thrombus formation in the microcirculation. *Toxicology*. 2010;269:148–154.
22. Kinzel L, Ernst A, Orth M, et al. A novel hsp90 inhibitor with reduced hepatotoxicity synergizes with radiotherapy to induce apoptosis, abrogate clonogenic survival, and improve tumor control in models of colorectal cancer. *Oncotarget*. 2016;7:43199–43219.
 23. Gonias SL, Campana WM. LDL receptor-related protein-1: a regulator of inflammation in atherosclerosis, cancer, and injury to the nervous system. *Am J Pathol*. 2014;184:18–27. doi: 10.1016/j.ajpath.2013.08.029.
 24. May P. The low-density lipoprotein receptor-related protein 1 in inflammation. *Curr Opin Lipidol*. 2013;24:134–137. doi: 10.1097/MOL.0b013e32835e809c.
 25. Strickland DK, Au DT, Cunfer P, Muratoglu SC. Low-density lipoprotein receptor-related protein-1: role in the regulation of vascular integrity. *Arterioscler Thromb Vasc Biol*. 2014;34:487–498. doi: 10.1161/ATVBAHA.113.301924.
 26. Kolaczowska E, Kubes P. Neutrophil recruitment and function in health and inflammation. *Nat Rev Immunol*. 2013;13:159–175. doi: 10.1038/nri3399.
 27. Ley K, Laudanna C, Cybulsky MI, Nourshargh S. Getting to the site of inflammation: the leukocyte adhesion cascade updated. *Nat Rev Immunol*. 2007;7:678–689. doi: 10.1038/nri2156.
 28. Nourshargh S, Alon R. Leukocyte migration into inflamed tissues. *Immunity*. 2014;41:694–707. doi: 10.1016/j.immuni.2014.10.008.
 29. Vestweber D. How leukocytes cross the vascular endothelium. *Nat Rev Immunol*. 2015;15:692–704. doi: 10.1038/nri3908.
 30. Denorme F, Wyseure T, Peeters M, Vandeputte N, Gils A, Deckmyn H, Vanhoorelbeke K, Declerck PJ, De Meyer SF. Inhibition of thrombin-activatable fibrinolysis inhibitor and plasminogen activator inhibitor-1 reduces ischemic brain damage in mice. *Stroke*. 2016;47:2419–2422. doi: 10.1161/STROKEAHA.116.014091.
 31. Wyseure T, Rubio M, Denorme F, Martinez de Lizarrondo S, Peeters M, Gils A, De Meyer SF, Vivien D, Declerck PJ. Innovative thrombolytic strategy using a heterodimer diabody against TAFI and PAI-1 in mouse models of thrombosis and stroke. *Blood*. 2015;125:1325–1332. doi: 10.1182/blood-2014-07-588319.
 32. Lau CL, Zhao Y, Kim J, Kron IL, Sharma A, Yang Z, Laubach VE, Linden J, Ailawadi G, Pinsky DJ. Enhanced fibrinolysis protects against lung ischemia-reperfusion injury. *J Thorac Cardiovasc Surg*. 2009;137:1241–1248. doi: 10.1016/j.jtcvs.2008.12.029.
 33. Nagai N, Suzuki Y, Van Hoef B, Lijnen HR, Collen D. Effects of plasminogen activator inhibitor-1 on ischemic brain injury in permanent and thrombotic middle cerebral artery occlusion models in mice. *J Thromb Haemost*. 2005;3:1379–1384. doi: 10.1111/j.1538-7836.2005.01466.x.
 34. Watanabe R, Nakajima T, Ogawa M, Suzuki J, Muto S, Itai A, Hirata Y, Nagai R, Isobe M. Effects of pharmacological suppression of plasminogen activator inhibitor-1 in myocardial remodeling after ischemia reperfusion injury. *Int Heart J*. 2011;52:388–392.
 35. Zaman AK, Fujii S, Schneider DJ, Taatjes DJ, Lijnen HR, Sobel BE. Deleterious effects of lack of cardiac PAI-1 after coronary occlusion in mice and their pathophysiologic determinants. *Histochem Cell Biol*. 2007;128:135–145. doi: 10.1007/s00418-007-0300-z.
 36. Gebbink RK, Reynolds CH, Tollefsen DM, Mertens K, Pannekoek H. Specific glycosaminoglycans support the inhibition of thrombin by plasminogen activator inhibitor 1. *Biochemistry*. 1993;32:1675–1680.
 37. Urano T, Serizawa K, Takada Y, Ny T, Takada A. Heparin and heparan sulfate enhancement of the inhibitory activity of plasminogen activator inhibitor type 1 toward urokinase type plasminogen activator. *Biochim Biophys Acta*. 1994;1201:217–222.
 38. Weckbach LT, Gola A, Winkelmann M, Jakob SM, Groesser L, Borgolte J, Pogoda F, Pick R, Pruenster M, Müller-Höcker J, Deindl E, Sperandio M, Walzog B. The cytokine midkine supports neutrophil trafficking during acute inflammation by promoting adhesion via $\beta 2$ integrins (CD11/CD18). *Blood*. 2014;123:1887–1896. doi: 10.1182/blood-2013-06-510875.
 39. Xu Z, Castellino FJ, Ploplis VA. Plasminogen activator inhibitor-1 (PAI-1) is cardioprotective in mice by maintaining microvascular integrity and cardiac architecture. *Blood*. 2010;115:2038–2047. doi: 10.1182/blood-2009-09-244962.
 40. DiStasi MR, Ley K. Opening the flood-gates: how neutrophil-endothelial interactions regulate permeability. *Trends Immunol*. 2009;30:547–556. doi: 10.1016/j.it.2009.07.012.
 41. Askari AT, Brennan ML, Zhou X, Drinko J, Morehead A, Thomas JD, Topol EJ, Hazen SL, Penn MS. Myeloperoxidase and plasminogen activator inhibitor 1 play a central role in ventricular remodeling after myocardial infarction. *J Exp Med*. 2003;197:615–624.
 42. Moriwaki H, Stempien-Otero A, Kremen M, Cozen AE, Dichek DA. Overexpression of urokinase by macrophages or deficiency of plasminogen activator inhibitor type 1 causes cardiac fibrosis in mice. *Circ Res*. 2004;95:637–644. doi: 10.1161/01.RES.0000141427.61023.f4.
 43. Eitzman DT, Westrick RJ, Nabel EG, Ginsburg D. Plasminogen activator inhibitor-1 and vitronectin promote vascular thrombosis in mice. *Blood*. 2000;95:577–580.
 44. Eren M, Painter CA, Atkinson JB, Declerck PJ, Vaughan DE. Age-dependent spontaneous coronary arterial thrombosis in transgenic mice that express a stable form of human plasminogen activator inhibitor-1. *Circulation*. 2002;106:491–496.
 45. Meltzer ME, Lisman T, de Groot PG, Meijers JC, le Cessie S, Doggen CJ, Rosendaal FR. Venous thrombosis risk associated with plasma hypofibrinolysis is explained by elevated plasma levels of TAFI and PAI-1. *Blood*. 2010;116:113–121. doi: 10.1182/blood-2010-02-267740.
 46. Fernandez-Cadenas I, Alvarez-Sabin J, Ribo M, Rubiera M, Mendioroz M, Molina CA, Rosell A, Montaner J. Influence of thrombin-activatable fibrinolysis inhibitor and plasminogen activator inhibitor-1 gene polymorphisms on tissue-type plasminogen activator-induced recanalization in ischemic stroke patients. *J Thromb Haemost*. 2007;5:1862–1868. doi: 10.1111/j.1538-7836.2007.02665.x.
 47. Thøgersen AM, Jansson JH, Boman K, Nilsson TK, Weinehall L, Huhtasaari F, Hallmans G. High plasminogen activator inhibitor and tissue plasminogen activator levels in plasma precede a first acute myocardial infarction in both men and women: evidence for the fibrinolytic system as an independent primary risk factor. *Circulation*. 1998;98:2241–2247.
 48. Suzuki Y, Nagai N, Collen D. Comparative effects of microplasmin and tissue-type plasminogen activator (tPA) on cerebral hemorrhage in a middle cerebral artery occlusion model in mice. *J Thromb Haemost*. 2004;2:1617–1621. doi: 10.1111/j.1538-7836.2004.00889.x.
 49. Fuchs TA, Brill A, Duerschmied D, Schatzberg D, Monestier M, Myers DD, Jr., Wroblewski SK, Wakefield TW, Hartwig JH, Wagner DD. Extracellular DNA traps promote thrombosis. *Proc Natl Acad Sci USA*. 2010;107:15880–15885.
 50. von Brühl ML, Stark K, Steinhart A, et al. Monocytes, neutrophils, and platelets cooperate to initiate and propagate venous thrombosis in mice in vivo. *J Exp Med*. 2012;209:819–835. doi: 10.1084/jem.20112322.
 51. Brown NJ, Agirbasli M, Vaughan DE. Comparative effect of angiotensin-converting enzyme inhibition and angiotensin II type 1 receptor antagonism on plasma fibrinolytic balance in humans. *Hypertension*. 1999;34:285–290.
 52. Vaughan DE, Rouleau JL, Ridker PM, Arnold JM, Menapace FJ, Pfeffer MA. Effects of ramipril on plasma fibrinolytic balance in patients with acute anterior myocardial infarction. HEART Study Investigators. *Circulation*. 1997;96:442–447.

Highlights

- Plasminogen activator inhibitor-1 (PAI-1) rapidly accumulates on the endothelium of the posts ischemic microvasculature.
- Deposited PAI-1 subsequently directs neutrophils to posts ischemic tissue by inducing affinity changes in integrins of these immune cells.
- PAI-1 causes affinity changes of neutrophil integrins via interaction with low-density lipoprotein receptor-related protein-1 and mitogen-activated protein kinases-dependent signaling pathways.
- PAI-1-dependent extravasation of neutrophils from the microvasculature to the reperfused tissue promotes microvascular leakage.
- Deficiency of PAI-1 effectively reverses ischemia-reperfusion injury without exhibiting side effects on microvascular hemostasis.